LC-DET-2012-066 at http://www-flc.desy.de/lcnotes

Results from a TPC Prototype for the Linear Collider Tracker with the MWPC and GEM Endplate Technologies

K. Ackermann[c], S. Arai[i], D.C. Arogancia[f], A.M. Bacala[f], M. Ball[a], T. Behnke[a], V. Eckardt[c], K. Fujii[l], N. Ghodbane[a], H.C. Gooc Jr.[f], T. Kijima[i], M. Hamann[a], M. Habu[i], R.-D. Heuer[b], K. Ikematsu[a], A. Kaukher[d], H. Kuroiwa[l], M.E. Janssen[a], Y. Kato[g], M. Kobayashi[l], T. Kuhl[a], T. Lux[b], T. Matsuda[l], A. Miyazaki[i], K. Nakamura[i], O. Nitoh[i], J. Pouthas[o], R.L. Reserva[f], Ph. Rosier[o], N. Sakamoto[h], T. Sanuki[j], R. Settles[c], A. Sugiyama[h], T. Takahashi[e], T. Watanabe[k], P. Wienemann[a], R. Wurth[a], M. Yamaguchi[h], A. Yamaguchi[m], T. Yamamura[j], H. Yamaoka[l], R. Yonamine[n]

[a] *DESY Hamburg, D-22607 Hamburg, Germany*
[b] *Universität Hamburg, D-22761 Hamburg, Germany*
[c] *Max-Planck-Institut für Physik, D-80805 Munich, Germany*
[d] *Universität Rostock, D-18051 Rostock, Germany*
[e] *Hiroshima University, Higashi-Hiroshima, Hiroshima 739-8526, Japan*
[f] *Mindanao State University, Iligan City 9200, Philippines*
[g] *Kinki University, Higashi-Osaka, Osaka 577-8502, Japan*
[h] *Saga University, Honjo, Saga 840-8502, Japan*
[i] *Tokyo University of Agriculture and Technology, Koganei, Tokyo 184-8588, Japan*
[j] *University of Tokyo, ICEPP, Tokyo 113-0033, Japan*
[k] *Kogakuin University, Hachiohji, Tokyo 192-0015, Japan*
[l] *KEK, IPNS, Tsukuba, Ibaraki 305-0801, Japan*
[m] *University of Tsukuba, Tsukuba, Ibaraki 305-8577, Japan*
[n] *Graduate University for Advanced Studies, KEK, Ibaraki 305-0801, Japan*
[o] *IPN, IN2P3 and Univ. de Paris-Sud, F-91405 Orsay, France*

Abstract

A Time Projection Chamber is being designed as central tracker for a detector at the linear collider. To provide a comparison and explore the potential improvements using Micro-Pattern Gas Detectors compared with Multi-Wire Proportional Chambers used up to now in TPCs, a small prototype chamber capable of being equipped with different gas-amplification techniques was built at MPI-Munich and exposed to cosmics in the 5 T magnet at DESY and subsequently to a testbeam in a 1 T magnet at KEK. The chamber was operated with four different endplate technologies during four beam periods in 2004–2005. This paper reports on the first and second tests using MWPC and GEM gas-amplification.

Some of the MWPC and the GEM results were published in the TIPP09 Proceedings [1]. *For the present paper, the data analysis technique has been improved significantly.* It also contains more information about the data-taking runs.

Keywords:
International Linear Collider (ILC), Compact Linear Collider (CLIC), Time Projection Chamber (TPC), Multiwire Proportional Chamber (MWPC), Micropattern Gas Detector (MPGD)
PACS: 29.40.Cs, 29.40.Gx

1. Introduction

A detector at the linear collider [2] will have a high-precision tracking system inside a calorimeter system, and both systems will have very high granularity. These will be contained in the detector solenoid which will produce the large magnetic field ($\sim$ 4T) needed to reduce backgrounds at the vertex and to enable very good momentum resolution.

There are two important aspects for tracking at the linear collider. The first is, as required by precision-physics measurements at the linear collider, that the detector must determine the momentum of charged tracks an order of magnitude more precisely than in previous experiments. The second aspect is that the detector must be optimized for the reconstruction of multi-jet final states. The jet-energy resolution using the particle-flow technique [3] is best when the reconstruction of individual particles in jets is as complete as possible, which means that efficiency in finding the charged and neutral particles should be as high as possible.

A Time Projection Chamber (TPC) is a candidate for the central tracker because of its very good performance in past collider experiments [4]. In order to obtain the order-of-magnitude improvement in momentum resolution and the highest possible track-recognition efficiency, the LCTPC groups [5] are pursuing R&D to find the best technology for the TPC.

2. The present series of R&D tests

TPCs have employed Multi-Wire-Proprotional-Chamber (MWPC) gas-amplification in previous large collider detectors [4]. The thrust of the R&D program [5][6][7] is to develop a TPC based on Micro-Pattern Gas Detectors (MPGDs) which promise to have better point and two-track resolution than wire chambers and to be more robust in high backgrounds. In the series of experiments in 2004-2005, several techniques were compared, gas amplification using MWPC, Micromegas (Micro-mesh gaseous structure)[8] and GEM (Gas Electron Multiplier)[9], and the resistive-anode technique[10].

To investigate the performance of these technologies, a small prototype chamber was built at MPI-Munich, initially with an MWPC endplate, tested using cosmics at DESY in a 5 T magnet and subsequently exposed in four test-beam runs at KEK using MWPC, GEM, Micromegas and resistive-anode endplates in a 1 T magnet. The chamber will be called MP-TPC, for MultiPrototype-TPC, in this paper. The runs were performed in the following order: MWPC (January-June 2004), GEM (April 2005), Micromegas (June 2005) and MPGD with resistive anode (October 2005). The Micromegas results have been published [11], and preliminary results for the different endplates have been shown at various workshops (see for example [12]).

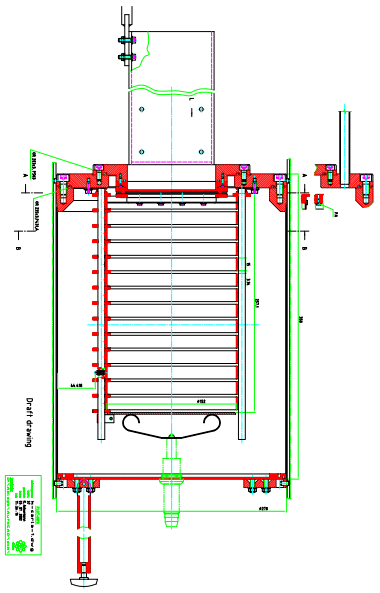

Figure 1: The MP-TPC prototype with MWPC anode. The cathode is at the bottom and the MWPC anode wires at the top. The 13 fieldcage potential rings which define the drift volume form the ladder-like pattern in the drawing. The fieldcage defines the TPC sensitive volume, and the whole structure is embedded in a cylindrical gas container which fit into in the 5 T magnet at DESY seen in Fig. 3 (upper).

The MWPC option had been kept as backup solution, since it as served well up to now, until the MPGD options had been more thoroughly understood. However, the new aspect that had to be measured for a TPC with MWPC endplate was how it behaves in a high magnetic field.

Some of the MWPC and GEM results using the MP-TPC were published earlier in the TIPP09 Proceedings [1]. The present paper contains more information about the data-taking runs; also the analysis method of the MWPC and GEM data has been improved.

The paper is organized as follows. The prototype with MWPC and GEM and the tests are described in the Sec. 3, the analyses in Sec. 4, results are presented in Sec. 5 and conclusions are drawn in Sec. 6.

3. The MP-TPC chamber

3.1. The MWPC prototype

The chamber with MWPC endplate used January-June 2004 is shown in Fig. 1. It has a sensitive length of 257 mm and sensitive diameter of 152 mm. Its outer diameter of 268 mm was dimensioned to fit into the superconducting 5 T magnet at DESY. The MWPC version of the MP-TPC had significantly reduced pad size, wires-to-pads and wire-to-wire spacing to improve the achievable point and two-track resolutions. The gas amplification occurred at the plane of anode sense wires with 20 μm diameter and spaced with 2 mm pitch. The sense-wire plane was placed 1 mm

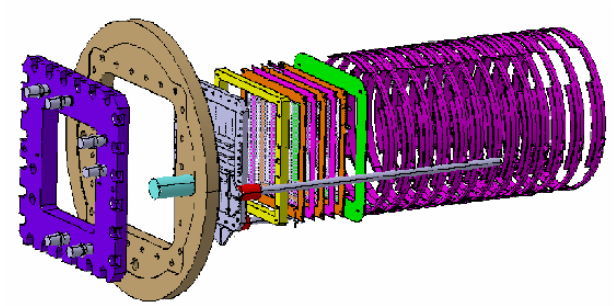

Figure 2: Blown-up view of the MP-TPC with triple-GEM. The three GEM layers are seen just to the left of the green guardring.

above the pad plane (2 mm–4 mm in previous TPCs). The pads with 2.3 mm×6.3 mm pitch covered the 10 cm×10 cm pad plane.

3.2. The GEM prototype

In December 2004, the MWPC plane was replaced by triple-GEM modules seen in the blown-up drawing of Fig. 2. For these tests the MP-TPC used gas-amplification provided by a three-layer stack of of CERN GEMs (50 μm thickness) with a spacing of 1.5 mm GEM-to-GEM and GEM-to-pads. The pad pitch was 1.27 mm×6.3 mm which covered the full 10 cm×10 cm pad plane. The GEMs were run at typically 320-335 V leading to amplification fields of ∼60 kV/cm and transfer/induction fields of ∼2 kV/cm.

3.3. Tests, Beamline, DAQ

3.3.1. The tests with cosmics at DESY and beam at KEK

The chamber with MWPC and readout electronics were initially commissioned at MPI-Munich and DESY and then installed in the 5 T solenoid as shown in the upper photograph of Fig. 3. This magnet has a bore diameter of 28 cm and length of 1 m and was equipped with a cosmic-ray trigger. Cosmic data was taken for B-fields between 0 T and 5 T.

After the cosmic runs at DESY, the chamber was transported to KEK where it was installed in the 1 T magnet, seen in the lower photograph of Fig. 3, which was situated in the $\pi 2$ beam line at the KEK 12-GeV PS. The 1 T Persistent Current solenoidal MAGnet (PCMAG) [13] has a bore diameter of 85 cm, length of 1.3 m and very thin coil windings with 20 % X_0 thickness.

3.3.2. The $\pi 2$ beamline

The $\pi 2$ beam provided a secondary beam of electrons, pions and protons with momenta up to 4 GeV/c derived from the PS beam incident on a Be target. The beam spill had a flat top of 1.5 s and a repetition rate of 0.25 Hz

The beam counters are shown in Fig. 4. Four scintillation counters were used with 4-fold coincidence to trigger the data acquisition. The first two (not shown in the figure) were placed just downstream of the beam slit which controlled the intensity while the second two were

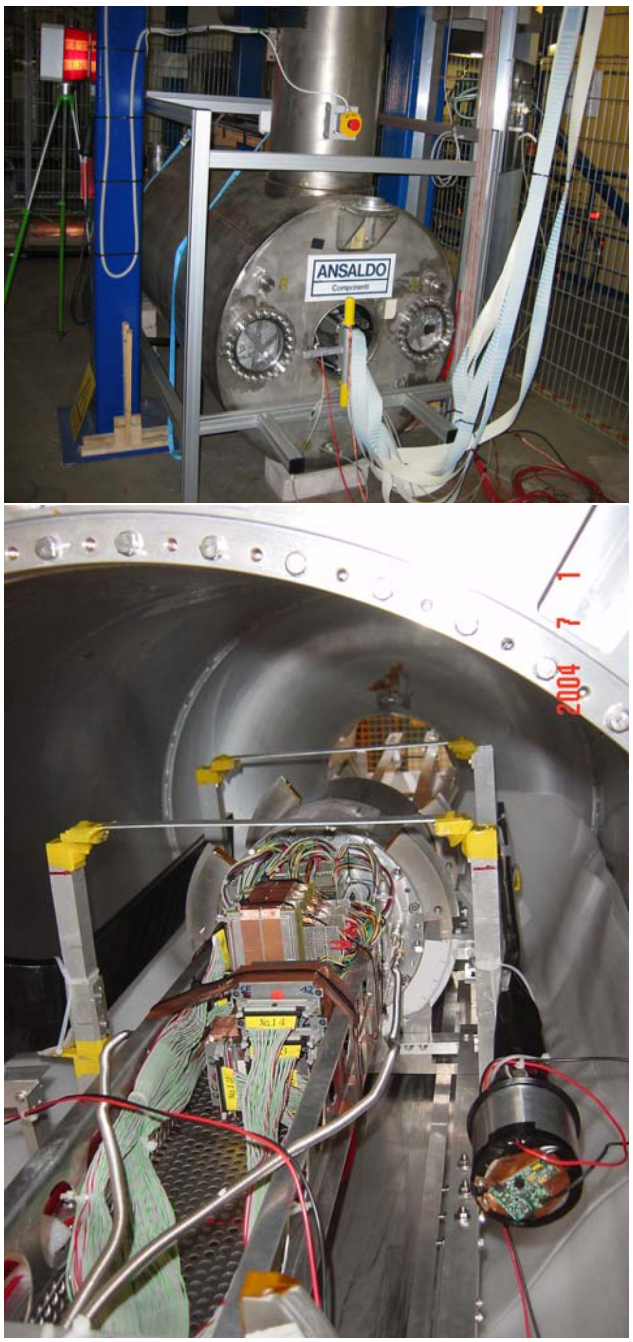

Figure 3: Upper: The MP-TPC inside the 5 T solenoid at DESY. Lower: The chamber inside the 1 T PCMAG at KEK.

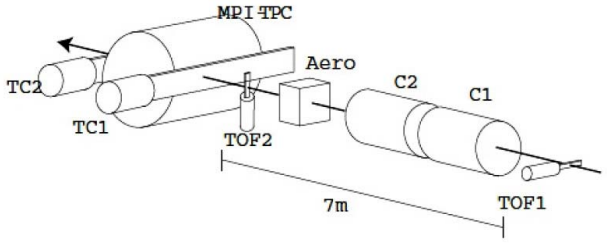

Figure 4: pi2 beam set up

located inside of PCMAG just upstream and downstream of the MP-TPC. These counters had an overlap region of $30 \times 10\,\mathrm{cm}^2$ to match the drift region of the chamber. Further details are covered in [11].

In addition, for the MWPC running there were two time-of-flight counters and one aerogel counter (n = 1.03) which allowed the particle identification of pions and protons at trigger level. These were employed for the dE/dx measurements described below. There were also two gas-Cherenkov counters for identification of electrons, which, however, were not included in the present analysis.

3.3.3. The DAQ system

The pads were read out with modules based on electronics developed for the TPC of the ALEPH experiment at LEP [14][15]. The pad signals were digitized by an eight-bit FADC running at a clock frequency of 12.5 MHz The electronics available for these tests was able to read out up to 384 pad channels. The DAQ system described in [11] contains additional information.

For the tests with MWPC, $\sim 2 \times 10^5$ cosmic triggers at DESY were registered for B=0 T, 1 T and 4 T, and $\sim 0.5 \times 10^5$ triggers under many different conditions were taken at KEK during the MWPC beam runs with B=0 T and 1 T.

During the June 2004 GEM data-taking in the $\pi 2$ beam, several different configurations of GEM gain and transfer/induction fields were tried out, again at B-fields of B=0 T and 1 T. The DAQ system collected a total of $\sim 10^5$ triggers with GEM.

4. Analyses

4.1. Theory

For a track perpendicular to the readout pad rows the spatial resolution attainable with the charge centroid method is given by the following formula:

$$\sigma^2_{\tilde{x}} = \int_{-\frac{1}{2}}^{+\frac{1}{2}} d\left(\frac{\tilde{x}}{w}\right)\left[[A] + \frac{1}{N_{\mathrm{eff}}}[B]\right] + [C] \qquad (1)$$

with

$$[A] := \left(\sum_a (a\,w)\ \langle F_a(\tilde{x}+\Delta x)\rangle - \tilde{x}\right)^2$$

$$[B] := \sum_{a,b} a\,b\,w^2\,\langle F_a(\tilde{x}+\Delta x)F_b(\tilde{x}+\Delta x)\rangle - \left(\sum_a a\,w\,\langle F_a(\tilde{x}+\Delta x)\rangle\right)^2$$

$$[C] := \left(\frac{\sigma_{\mathrm{E}}}{\bar{G}}\right)^2 \left\langle \frac{1}{N^2}\right\rangle \sum_a (a\,w)^2,$$

where N_{eff} is the effective number of seed electrons defined by

$$N_{\mathrm{eff}} := \left[\left\langle\frac{1}{N}\right\rangle\left\langle\left(\frac{G}{\bar{G}}\right)^2\right\rangle\right]^{-1}, \qquad (2)$$

w the pad pitch, G the gas gain, $\bar{G}$ its average, N the number of seed electrons, σ_{E} the electronic noise per readout pad, and a and b the pad indices running over the pads with signal charge.

The first term in Eq.(1) involving $[A]$ corresponds to the well known S-shape systematics, which is purely geometric and independent of the number of primary electrons. This term vanishes in the narrow pad limit, $w \to 0$, while it approaches the famous $(w/\sqrt{12})^2$ in the wide pad limit, $w \gg \sigma_{\mathrm{d}}$, σ^0_{PR} – see Eqs.(3) and (5) below. The second term involving $[B]$ can be interpreted as the combined effect of the diffusion, the gas gain fluctuations, and the finite width of the readout pads. This term scales as $1/N_{\mathrm{eff}}$ and vanishes at $z = 0$. The last term $[C]$ represents the contribution from the electronic noise and is independent of the shape of the pad response function or the diffusion. It scales as $(w\,\sigma_{\mathrm{E}}/\bar{G})^2\,\langle 1/N^2\rangle$.

Since the $[B]$ contribution vanishes at $z = 0$ and since the $[C]$ term is negligible in this case, the $[A]$ contribution at $z = 0$ can read from the resolution plot and σ_0 estimated using Eq. (9) below.

The pad response function $F_a(x)$ only appears in the following two forms:

$$\langle F_a(\tilde{x}+\Delta x)\rangle := \int d\Delta x\, P_{\mathrm{D}}(\Delta x;\sigma_{\mathrm{d}})\, F_a(\tilde{x}+\Delta x)$$

and

$$\langle F_a(\tilde{x}+\Delta x)F_b(\tilde{x}+\Delta x)\rangle := \int d\Delta x\, P_{\mathrm{D}}(\Delta x;\sigma_{\mathrm{d}})\, F_a(\tilde{x}+\Delta x)\, F_b(\tilde{x}+\Delta x),$$

where the probability distribution function for diffusion, $P_{\mathrm{D}}(\Delta x;\sigma_{\mathrm{d}})$, is given by

$$P_{\mathrm{D}}(\Delta x;\sigma_{\mathrm{d}}) := \frac{1}{\sqrt{2\pi}\,\sigma_{\mathrm{d}}}\exp\left[-\frac{1}{2}\left(\frac{\Delta x}{\sigma_{\mathrm{d}}}\right)\right] \qquad (3)$$

with $\sigma^2_{\mathrm{d}} = C^2_{\mathrm{D}} z$. The two forms can be numerically evaluated, once the functional form of $F_a(x)$ is given.

The pad response function $F_a(x)$ can readily be calculated if the normalized signal charge density at x',

$f(x'-x)$, on the readout pads is known for a line charge arriving at the position x of the readout module:

$$F_a(x) \quad = \quad \int_{x' \in \text{pad } a} dx'\, f(x'-x). \tag{4}$$

For MWPC, $f(x'-x)$ is the electrostatically induced charge on the pad plane by a point-like avalanche at the anode wire. For GEM, $f(x'-x)$ is mostly determined by the diffusion after the seed electrons reach the amplification region and can be approximated by a Gaussian:

$$f(x'-x) \quad = \quad \frac{1}{\sqrt{2\pi}\,\sigma^0_{\rm PR}} \exp\left[-\frac{1}{2}\left(\frac{x'-x}{\sigma^0_{\rm PR}}\right)^2\right] \tag{5}$$

where $\sigma^0_{\rm PR}$ is the diffusion after reaching the amplification region.

4.2. Resolution studies

The equations and parameters for the studies follow from Sec. 4.1. The diffusion constant $C_{\rm D}$ is important for the single-point and two-track resolutions and was measured using the behaviour of signal-charge spread as a function of drift distance z. In the asymptotic regeme where $\sigma_{\rm d}/w \gtrsim 0.5$, the r.m.s. of the charge spread or induced-charge spread is parametrized by

$$\sigma^2_{\rm PR}(z) = \sigma^2_{\rm PR}(0) + C^2_{\rm D} \times z, \tag{6}$$

and the point resolution by

$$\sigma^2_x(z) = \sigma^2_0 + C^2_{\rm D}/N_{\rm eff} \times z. \tag{7}$$

The width $\sigma_{\rm PR}(0)$ of the MWPC signal induced on the pads at $z = 0$ is related to geometrical properties at the wire-chamber cell: wire pitch, pad–wire distance and pad size.

In the case of GEM, $\sigma_{\rm PR}(0)$ is the real charge spread and depends mainly on the induction field gradient and spacing which determine the diffusion spreading of the charges arriving at the pads, and on the pad pitch w:

$$\sigma^2_{\rm PR}(0) = (\sigma^0_{\rm PR})^2 + w^2/12. \tag{8}$$

The point resolution σ_0 is related to signal-to-noise of the electronics and to the S-shape systematics and/or the hodoscope effect at $z = 0$.

$$\sigma^2_0 = [C] + \frac{1}{N_{\rm eff}} \int_{-1/2}^{+1/2} d\left(\frac{\tilde{x}}{w}\right) [A](z=0) \tag{9}$$

The quantity $N_{\rm eff}$, the effective number of electrons contributing to the resolution, is explained in Eq.(2) and depends on several quantities. These quantities are also affected by the crossing-angles of the projected track relative to the pads and, in the case of MWPC, relative to the wires.

The charge width was derived from a Gaussian fit to the distribution of charge around the center-of-gravity of a hit. The point resolution was calculated using the Double-Fit program [17] in which standard deviations of hits for a pad row are calculated twice with respect to track-fits ("Double-Fit"), first with and second without the given pad row. The correct point resolution is the geometric mean of the standard deviations of hits with respect to the two fits [18].

Equations (6) and (7) represent the ideal situation and give reasonable agreement with the measurements for a TPC with MPGD gas amplification [11][16]. In the MWPC case, however, $E \times B$ effects are important as will be seen next in Sec. 5.1.

5. Results

5.1. MWPC endplate

The gas used was the so-called TDR gas[3], Ar-CH_4-CO_2 (93:5:2)%. The chamber was operated at atmospheric pressure; the pressure and the ambient temperature were continuously monitored. The drift velocity was measured to be $4.52\pm0.04\,\text{cm}/\mu\text{s}$ at the drift field of $220\,\text{V/cm}$ during the beam runs.

Charge spread and point resolution

The cosmic data at B = 0 T, 1 T and 4 T will be compared with $4\,\text{GeV/c}$ π^- beam data at 0 T and 1 T magnetic fields. After the data was corrected for dead channels and edge effects, the tracking efficiency was essentially 100%.

Angle cuts of (polar, azimuthal)=($\pm5^o$, $\pm4^o$) were applied to the cosmic data to obtain a sample with track directions for comparison with the beam data within cuts of (polar, azimuthal)=($\pm2^o$, $\pm3^o$). The final samples selected for the diffusion and point-resolution comparisons contained about 2×10^4 tracks in the cosmic data and 10^4 tracks in the beam data.

The main question to be answered was on the behavior of the MWPC data at 4 T; plots are shown in Figs. 5, 6, and 7. A dotted line indicates the fit and range for the simple formulae, Sec. 4.2, and a solid line shows a simulation using Magboltz [24].

The fits to the data yield the parameters with statistical errors in Table 1. The statistical errors are seen to be quite small.

Runs	B(T)	$N_{\rm track}$	$C_{\rm D}$	$\sigma_{\rm PR}(0)$	$\frac{C_{\rm D}}{\sqrt{N_{\rm eff}}}$	σ_0
Cosmics	0	6k	491±2	1120±6	126± 4	181±19
Cosmics	1	5k	226±2	1240±4	54± 3	206±11
Cosmics	4	9k	73±10	1440±8	0±14	300± 5
Beam	0	5k	466±1	1340±3	117± 3	179±12
Beam	1	5k	212±1	1290±1	48± 2	182± 7

Table 1: Parameters with statistical errors as fit to the data. The units are $\mu\text{m}/\sqrt{\text{cm}}$ for $C_{\rm D}$ and μm for $\sigma_{\rm PR}(0)$ and σ_0.

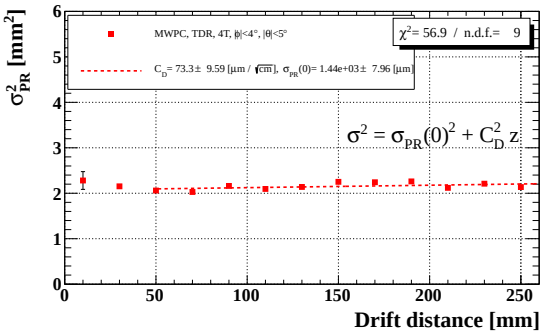

Figure 5: Diffusion results at 4 T for DESY cosmics.

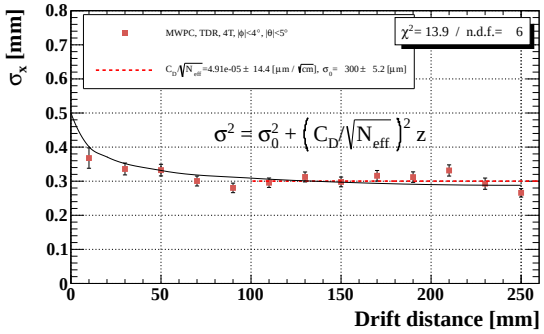

Figure 6: x Point-resolution results at 4 T for DESY cosmics.

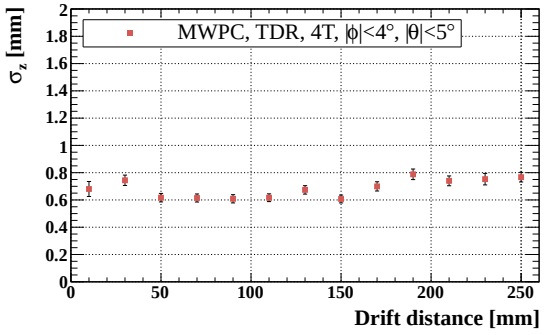

Figure 7: z resolution for cosmic data at DESY at 4 T

The data at 0 T and 1 T for the charge width $\sigma_{\rm PR}(z)$ and the point resolution $\sigma_x(z)$ from the DESY cosmic and KEK beam runs were found to agree to somewhat better than $\sim 10\%$, which is quite reasonable given the very different data-taking environments. Therefore, the systematic effects will taken be into account by simply using $\pm 5\%$ of the central value as systematic error, also for 4 T. The resulting combined fits are given in Table 2, where the statistical error has been added in quadrature to the $\pm 5\%$ systematic error.

B(T)	$C_{\rm D}$	$\sigma_{\rm PR}(0)$	$\frac{C_{\rm D}}{\sqrt{N_{\rm eff}}}$	σ_0
0	471±24	1296±75	120±60	180±24
1	215± 6	1287±64	50± 6	189±16
4	73±11	1440±72	0±14	300±16

Table 2: Averaged results with total errors for the MWPC data. The units are $\mu{\rm m}/\sqrt{\rm cm}$ for $C_{\rm D}$ and μm for $\sigma_{\rm PR}(0)$ and σ_0.

Discussion

In the case of Fig. 5, the measured $C_{\rm D}$ values predicted by Magboltz [24] agree with the measured values in Table 2 at 0 T, 1 T and 4 T, namely 440, 200 and 60 $\mu{\rm m}/\sqrt{\rm cm}$ respectively.

The prediction for B = 4 T is of particular interest for the linear collider and has been confirmed now by the present and earlier by other experiments [25][26].

The resolution curve at small z in Fig. 6 is indicative of the declustering effect [1] [22] [23].

5.1.1. Angle effect

To measure the angular dependence, the MP-TPC was rotated by angles ϕ with respect to the beam direction of $\phi \approx \pm 10^0$ and $\pm 20^0$ and exposed for roughly 10^3 triggers to the π beam at 4 GeV/c. The results [19] for $\sigma_{\rm PR}(0)$ are shown in Fig. 8. The shape of this curve is a measure of the pad-angle effect and is proportional to $\frac{h \cdot \tan(\varphi - \varphi_{min})}{\sqrt{12}}$, where h is the pad height.

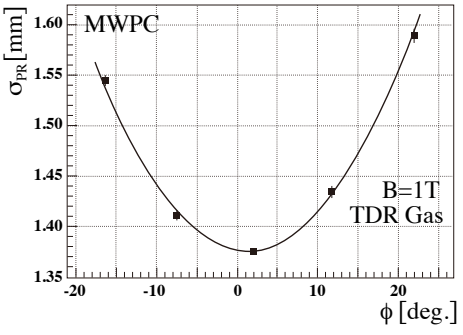

Figure 8: Angle dependence of the pad response.

5.1.2. dE/dx studies

The trigger elements are described in Sec. 3.3.2. The proton and π^- at 1, 2 and 4 GeV/c were used for the dE/dx results [20][21]. The upper three distributions of Fig. 9 show the dE/dx results, and the lowest distribution shows the measured $\beta\gamma$ dependence of dE/dx.

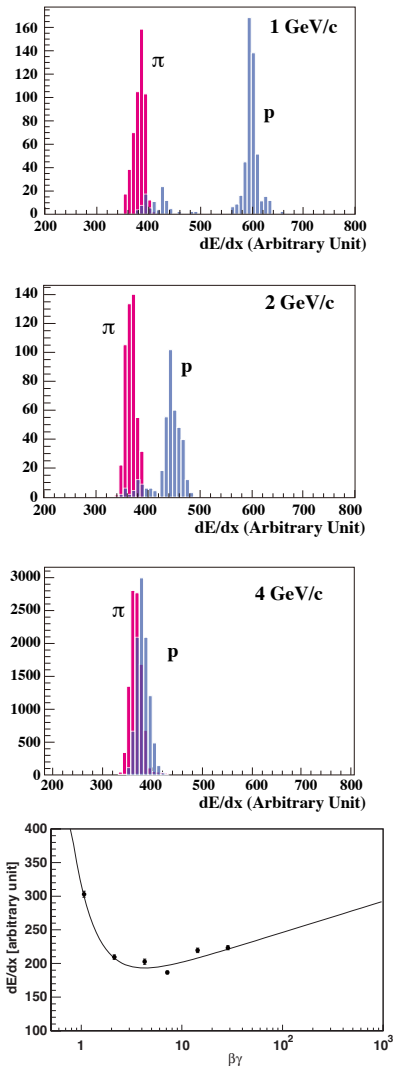

Figure 9: Measured dE/dX-distributions (upper three) and $\beta\gamma$ dependence (lowest).

The dE/dx accuracy was found to be between 22% and 27% for the MP-TPC. When extrapolated to the size of the LCTPC, these correspond to an accuracy of 3.6% to 4.2%. Thus an important TPC by-product for the linear collider physics analyses, the dE/dx performance for particle identification, has been verified at these test-beam runs.

5.2. **GEM endplate**

The gases used were the TDR gas[3], Ar-CH_4-CO_2 (93:5:2)%, and P5, Ar-CH_4 (95:5)%. The chamber was again operated at atmospheric pressure, and the pressure and the ambient temperature were continuously monitored. The TDR drift velocity measurement is seen Sec. 5.1. For P5, it was measured to be 4.16±0.04 cm/μs at a drift field of 100 V/cm during the tests.

Charge spread and point resolution

The 4 GeV/c π^- beam data at 0 T and 1 T magnetic fields are used for this section. As in the MWPC case, after the data was corrected for dead channels and edge effects, the tracking efficiency was essentially 100%. The final samples selected for the diffusion and point-resolution comparisons contain about 10^5 tracks.

The angular cuts on the beam data are (polar, azimuthal)=($\pm 3^o$, $\pm 2^o$) for the TDR gas and (polar, azimuthal)=($\pm 3^o$, $\pm 3.5^o$) for P5. The plots of Fig. 10 compare the charge width σ^2_{PR} versus z for for the TDR gas at 1 T and P5 gas at 1 T magnetic field and Fig. 11 shows the point resolution σ_x versus z for the two gases. A dotted line indicates the fit and range for the simple formulae, Sec. 4.2, and a solid line represents the theory, Sec. 4.1.

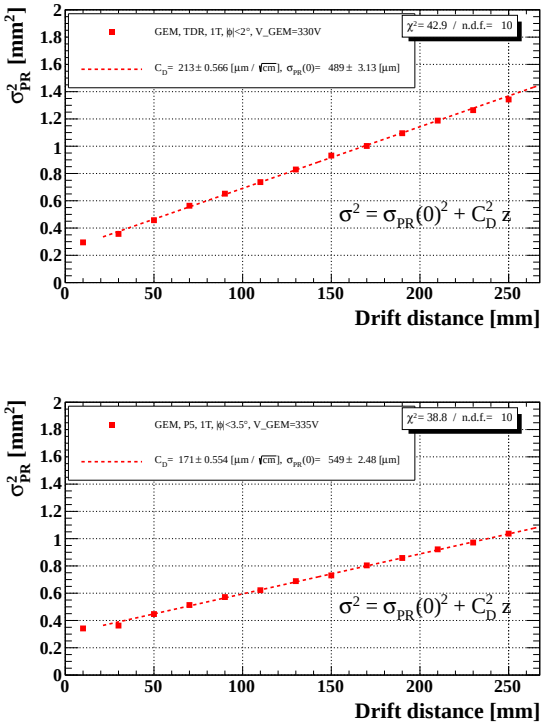

Figure 10: Diffusion results for the TDR (upper) and P5 (lower) gases.

The fits to the data yield the parameters in Table 3. The statistical errors are very small as they were in the MWPC case. Using ±5% of the central value as systematic error

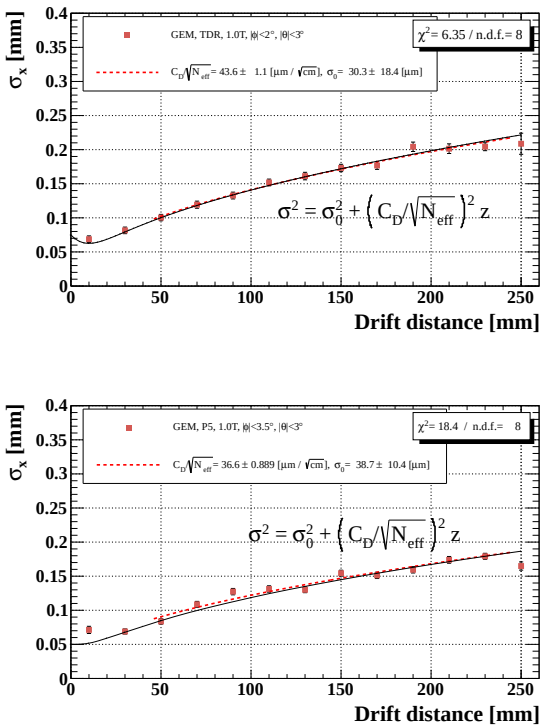

Figure 11: x Point-resolution results for the TDR (upper) and P5 (lower) gases.

as in the MWPC case, the results with the total errors for the GEM runs are found in Table 4. The diffusion constants agree with predictions by Magboltz: 200, 730, 160 $\mu\mathrm{m}/\sqrt{\mathrm{cm}}$ for TDR (1 T), P5 (0 T), P5 (1 T), respectively.

Runs	B(T)	N_{track}	C_{D}	$\sigma_{\mathrm{PR}}(0)$	$\frac{C_{\mathrm{D}}}{\sqrt{N_{\mathrm{eff}}}}$	σ_0
TDR	1	5k	213±0.6	489± 3	44±1.1	30± 18
P5	0	4k	741±2.8	598±15	178±3.0	0±117
P5	1	4k	171±0.6	549± 3	37±0.9	39± 10

Table 3: Parameters with statistical errors as fit to the data.

Runs	B(T)	C_{D}	$\sigma_{\mathrm{PR}}(0)$	$\frac{C_{\mathrm{D}}}{\sqrt{N_{\mathrm{eff}}}}$	σ_0
TDR	1	213±11	489±25	44± 3	30± 18
P5	0	741±37	598±33	178± 9	0±117
P5	1	171± 9	549±28	37± 2	39± 10

Table 4: Parameters with the total errors. The units are $\mu\mathrm{m}/\sqrt{\mathrm{cm}}$ for C_{D} and μm for $\sigma_{\mathrm{PR}}(0)$ and σ_0.

Before concluding, it should be said that the z resolution results were determined for all data sets, and were consistent with $\sim$0.3–0.8 mm in all cases. Figure 7 is an example of this measurement.

6. Conclusions

The MWPC point resolution is unfavorably affected by E×B effects for large magnetic field, as clearly seen in Fig. 6. With MWPC the point error measured at 4 T is about a factor three larger than the goal for the LCTPC [6][7], so that the previously successful MWPC technology in past experiments is no longer considered to be a fall-back option for the TPC at the linear collider.

In contrast, the GEM point resolutions for the two gases are very good at 1 T B-field (Table 3) and within the goals for the LCTPC [6][7]. Therefore the GEM technology is a viable option for the linear collider central tracker.

References

[1] K. Ackermann et al.,*Cosmic Ray Tests of the Prototype TPC for the ILC Experiment*, arXiv:0905.2655v1, published in TIPP09 Proceedings, Nucl. Instr. and Meth. A623(2010)1-646.

[2] The GDE (Global Design Effort) submitted the initial design for the complete ILC machine in 2007. This "Reference Design Report" is available at http://www.linearcollider.org/rdr. A second iteration on the design is underway and will be released as TDR in 2012.
The CLIC (Compact Linear Collider) machine is being investigated at CERN as a way to reach higher energies: http://www.cern.ch/clic.

[3] TESLA Technical Design Report, DESY 2001-011, ECFA 2001-209, March 2001.

[4] M.T. Ronan, *Time-projection chambers*, p.264 of the PDG Particle Physics Booklet July 2004. For a thorough overview of TPC applications, see
`http://instrumentationcolloquium.lbl.gov /Time_Projection_Chamber_R&D.pdf`.

[5] The latest updates may be found on the LCTPC website. `//http://www.lctpc.org/`.

[6] The TPC status report to the Tracking Review by the WWS R&D Panel at the ACFA LC workshop in Beijing, February 2007, included a complete overview of the groups, of design issues for the LCTPC and of the R&D work to address the issues. It is published as LC Note LC-DET-2007-005 at `http://flcweb01.desy.de/lcnotes`.

[7] Proposal PRC R&D-01/03, DESY Physics Review Committee October 2001, published as LC Note LC-DET-2002-008 at `http://flcweb01.desy.de/lcnotes`. See `http://www.desy.de/f/prc/` for the October 2001, May 2003, November 2005, May 2006, April 2008 and October 2010 R&D status reports.

[8] Y. Giomataris et al., *MicroMegas: A High Granularity Position Sensitive Gaseous Detector for High Particle Flux Environments*, Nucl. Instr. and Meth. A376(1996)29.

[9] F. Sauli, *GEM: A New Concept for Electron Amplification in Gas Detectors*, Nucl. Instr. and Meth. A386(1997)531.

[10] M. Dixit et al., Nucl. Instr. and Meth. A518(2004)721. See also `www.physics.carleton.ca/research/ilc/tpc.html`.

[11] D. C. Arogancia et al., *Study in a beam test of the resolution of a Micromegas TPC with standard readout pads*, Nucl. Instr. and Meth. A 602 (2009) 403.

[12] M. Kobayashi et al., Nucl. Instr. and Meth. A581(2007)265 and references therein.

[13] Y. Ajima et al., *A superconducting solenoidal spectrometer for a ballon-borne experiment*, Nucl. Instr. and Meth. A443(2000)71.

[14] M. Ball, N. Ghodbane, M. Janssen and P. Wienemann, *A DAQ System for Linear Collider TPC Prototypes based on the ALEPH TPC Electronics*, LC-DET-2004-013 at `http://flcweb01.desy.de/lcnotes`.

[15] C. Bowdry, ed., The Aleph Handbook (1995), ISBN 92-9083-072-7, publ. by CERN 1995.

[16] M. Kobayashi, *An estimation of the effective number of electrons contributing to the coordinate measurement of a TPC*, Nucl. Instr. and Meth. A562(2006)136.

[17] M.E. Jannsen, *Auflösungsstudien an einer Zeit-Projektions-Kammer (TPC) mit GEM-Gasverstärkungssystem*, Diplomarbeit U.Dortmund, DESY-THESIS-2004-049, September 2004.

[18] This application of the geometric-mean for this measurement has been used for several years; a recent proof is given in the appendix of Ref. [11].

[19] K. Nakamura, thesis, Tokyo University of Agriculture and Technology.

[20] S. Arai, *Measurement of energy loss by charged particles with a Time Projection Chamber*, Diploma thesis 2005, Tokyo U. of Agriculture and Technology, Japan.

[21] R.L. Reserva, presented at the LCWS2005, Stanford University.

[22] W. Blum, U. Stiegler, P. Gondolo and L. Rolandi, Nucl. Instr. and Meth. A252(1986)407.

[23] S.R. Amendolia et al., *The spatial resolution of the ALEPH TPC*, Nucl. Instr. and Meth. A283(1989)573-577.

[24] S.F. Biagi, Nucl. Instr. and Meth. A283(1989)716.

[25] J. Kaminski et al., *Development and studies of a time projection chamber with GEMs*, Nucl. Instr. and Meth. A535(2004)201-205.

[26] D. Karlen et al.,*TPC performance in magnetic fields with GEM and pad readout*, Nucl. Instr. and Meth. A555(2005)80-92.